VNU Journal of Science: Mathematics - Physics

Journal homepage: https://js.vnu.edu.vn/MaP

Original Article

Effect of Annealing Temperature on Photoluminescence Emission and Photocatalytic Activity of Hydrothermal ZnO Nanorods

Nguyen Xuan Sang*

Department of Electronics and Telecommunication, Saigon University, 273 An Duong Vuong, Ward 3, District 5, Ho Chi Minh City, Vietnam

Received 18 November 2018
Revised 08 January 2019; Accepted 20 January 2019

Abstract: This work reports photoluminescence evolution of hydrothermally homogeneous ZnO nanorods under thermal annealing at various temperatures. The crystalline structure and morphology of synthesized samples were characterized by X-ray diffractometry and Scanning Electron Microscopy. The optical properties induced by defect state transitions were investigated by photoluminescence emission. Besides defect states induced emissions in the visible range, the photocatalytic activity of annealed samples was evaluated which indicated that the higher visible photoluminescence intensity gives the better catalytic activity.

Keyword: ZnO nanorod, thermal treatment, photoluminescence, photocatalyst.

1. Introduction

With a wide bandgap (3.37 eV) and large exciton binding energy (60 meV) at room temperature, ZnO is one of the most interesting oxide semiconductors which has received huge attention from scientists worldwide in many application aspects such as ultraviolet (UV) laser, white light emitting diode (LED), photocatalyst, and sensor [1-3]. Depending on fabrication technique, many types of nano-sized ZnO morphology could be obtained such as nanoparticle, nanowire, micro/nanorod, microdisk. In semiconductor technology and application, one-dimensional ZnO nanostructure such as

*Corresponding author.
E-mail address: sangnguyen@sgu.edu.vn

https//doi.org/ 10.25073/2588-1124/vnumap.4299

nanowire, nanorod is technically important due to the unipolar characteristics which could play a crucial role as interconnects in nanoscale electronic devices.

Among various synthesis means, the hydrothermal method is a cheap, safe and friendly-user technique which could easily fabricate uniform ZnO nanostructures. Hence, in this study, ZnO nano/microrods were one-pot hydrothermally synthesized, then thermal annealing treatment was carried out directly at different temperatures. Crystalline structure and morphology of fabricated samples were characterized by X-ray diffractometric (XRD) and Scanning Electron Spectroscopy (SEM). Photoluminescence (PL) emission was investigated at room temperature with an excitation wavelength of 325 nm. The photocatalytic activity of annealed ZnO samples was evaluated by UV-Vis (HACH 5000) system measuring the degradation of methylene blue in solution under natural sunlight irradiation.

2. Chemicals and fabrication process

Zinc acetate dihydrate ($Zn(CH_3COO)_2.2H_2O$, 99% Merck), Sodium hydroxide (NaOH, 99% Merck) and Hexamethylenetetramine (HMTA, Merck), bi-distilled water were purchased and/or used without further purification. The synthesis procedure was started with two solutions of NaOH 8g and $Zn(Ac)_2$ 4.39g obtained in distilled water 50 ml. Then these solutions were mixed in the presence of hexamethylenetetramine (HMTA) 0.024g at room temperature in 30 min of magnetic stirring. The clear solution was poured into a Teflon-lined autoclave and hydrothermally heated at 150°C for 8 h. The autoclave was naturally cooled to room temperature (RT) and the white precipitate was washed with distilled water until pH reaches 7. Then, the powder was dried at 100°C overnight. Finally, these samples were annealed at 400°C, 700°C, and 900°C named as ZnO400, ZnO700 and ZnO900, respectively.

3. Results and discussion

3.1. Structural and morphological analysis

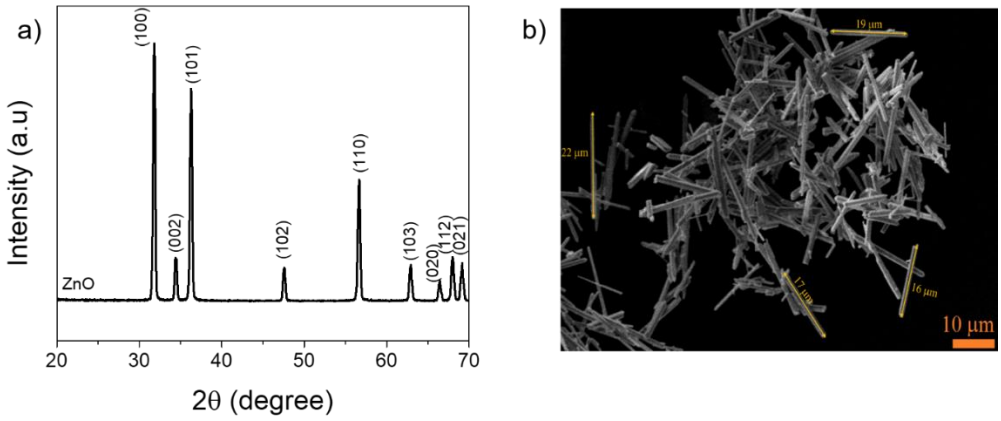

Figure 1. Structure and morphology characterizations: a) XRD patterns, b) SEM image.

The crystal structure and morphology of the synthesized ZnO microstructures were carried out *via* X-ray diffraction (XRD) and SEM, as shown in Fig. 1a, b, respectively. The main diffraction peaks implied that produced powders were highly single-phase hexagonal wurtzite structure, with average crystal size being 27.11 nm and lattice constants of a = 0.3249 nm and c = 0.5212 nm. This result is in the good agreement with JCPDS 36-1451 card [4]. There was no other peak of impurities observed. In addition, according to Fig. 2b, the SEM images showed that the morphology of ZnO was homogeneously uniform rod-like shape with length of 16.0 – 22.0 μm and dimension ranged from 0.8 to 1.6 μm.

3.2. Photoluminescence analysis

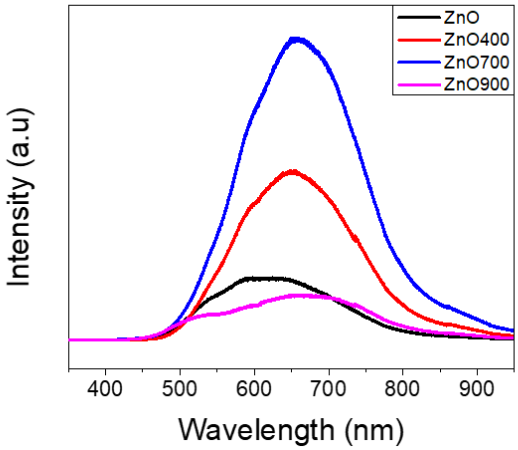

Figure 2. Room temperature photoluminescence emission of synthesized samples.

Photoluminescence is a suitable and nondestructive technique in order to determine radiative transitions in the band gap. In this study, PL measurements were performed at room temperature. In principle, the UV peak in the PL spectrum, at around 380 nm (3.26 eV) is related to the emission from the conduction band to the valence band. When as-prepared ZnO treated at different temperatures, ZnO400, ZnO700 and ZnO900, no UV peaks were observed in these samples. Besides the UV emission peak, visible emissions also are important as they relate to defect level transition in the material. Popular intrinsic defects in ZnO are zinc vacancies (V_{Zn}), zinc interstitials (Zn_i), oxygen vacancies (V_O), oxygen interstitials (O_i) and their ionized states. In this study, visible bands were strongly observed ranged from 500 to 900 nm. In general, the as-prepared ZnO had two peaks at 597 nm (2.08 eV) and 635 nm (1.95 eV), while for the ZnO400 sample one peak at 654 nm (1.90 eV), for the ZnO700 sample: 660 nm (1.88 eV) and for the ZnO900 sample: 514 nm (2.41 eV) and 650 nm (1.9 eV) peaks have been observed (Fig. 2). When the annealing temperature increased from 400℃ to 700℃, the emission intensity increased. On the contrary, the 900℃ annealed sample has the lowest visible emission intensity. From these results, it could be concluded that the thermal treatment had a great influence on the types and concentration of defects in ZnO nanostructures. Annealing process in the air could absorb oxygen on the surface of ZnO and brought ZnO into O-rich condition. Janotti *et al.*[5] suggested that zinc vacancies which act as deep acceptors can more easily form in *n*-type samples, due to its low formation energy, and particularly favorable in oxygen-rich conditions. In

addition, excess oxygen atoms from air could be accommodated in the form of oxygen interstitial. Thus, contents of oxygen-related defects in annealed samples such as oxygen interstitial, and oxygen vacancy would be increased through thermal treatment at high temperature. The thermodynamic transition for native defects in ZnO based on Janotti calculation was shown in Figure 3.

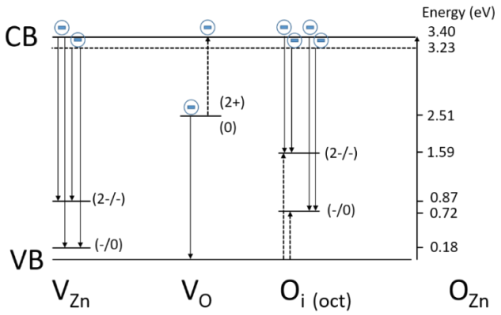

Figure 3. Transition levels for intrinsic defects in ZnO [5].

To further investigate the intrinsic defects in synthetic ZnO samples by hydrothermal method and treated at different temperatures, Gaussian-resolved method was used for the visible bands in the PL spectrum. Results were shown in Figure 4.

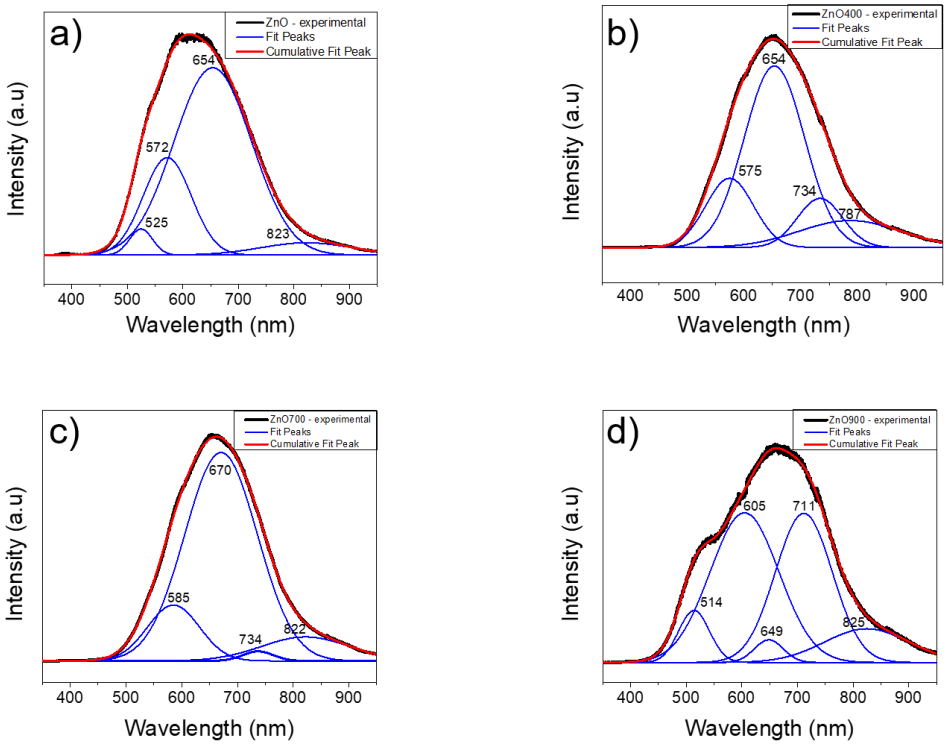

Figure 4. Photoluminescence spectra of: a) ZnO, b) ZnO400, c) ZnO700 and d) ZnO900.

Firstly, the green emission was observed in deep-level (DL) region at 525 nm (2.36 eV) and 514 nm (2.41 eV), respectively, in samples ZnO and ZnO900 (Fig. 4a and d). According to studies by Vanheusden [6,7], the correlation between the intensity of the green luminescence and the concentration of V_O based on the observation of a line with $g \sim 1.96$ in EPR measurement proposed for this emission. In addition, Leiter [8, 9] reported the green band around 2.45 eV with oxygen vacancies based on optically detected magnetic resonance experiments. Still, in the debate, Reynolds [10] and Kohan [11] have suggested that transition between the conduction band (or shallow donor) and the V_{Zn} are the sources of green band. Based on Janotti's calculation [5], this transition would give rise to luminescence at around 2.4 – 2.5 eV. Moreover, a strong argument in favor of zinc vacancies had been provided by strong passivation of the green emission by hydrogen plasma treatment in experiments of Sekiguchi [12] and Lavrov [13] who simultaneously observed an increase in vibrational modes associated with hydrogenated zinc vacancies. Hydrogen atoms as a donor passivated zinc vacancies which were reported as deep acceptors by forming O-H chemical bonds [13]. Secondly, due to the precursors ratio of Zn^{2+}:OH^- = 1:10, ZnO itself was in the oxygen-rich condition and then, the annealing in air also may inject additional oxygen into the ZnO lattice. Thus, defects as excess oxygen [14, 15], O_i [16] or other complex defects [15, 17] were attributed to the yellow–orange emissions which were appeared in all samples and red-shifted with increasing the annealing temperature, i.e. 572 nm (2.17 eV), 575 nm (2.16 eV), 585 nm (2.12 eV) and 605 nm (2.05 eV) in ZnO, ZnO400, ZnO700 and ZnO900 respectively. Furthermore, the dominant emission peaks appeared in ZnO samples were in the red region at 654 nm (1.90 eV) in ZnO and ZnO400, 670 nm (1.85 eV) in ZnO700 would possibly be attributed to $O_{i(oct)}^{2-}$ defect [5]. Thirdly, the radiative recombination of shallow donor with deep acceptor O_i could give rise to the NIR luminescence at 734 nm (1.69 eV) in ZnO400 and ZnO700, 711 nm (1.74 eV) in ZnO900 [18]. In this study, we also obtained an infrared emission. This peak occurs in as-prepared ZnO and ZnO treated at relatively high temperatures (ZnO700, ZnO900). We assumed that this emission might be assigned to $O_{i\ (oct)}$. However, yellow – orange, red and other emissions appeared at shorter wavelength region are required further investigation.

Table 1. Summarized percentages of the PL spectra of ZnO nanostructures annealed at different temperatures de-convoluted by Gaussian distribution.

Portion of defect contribution (%)					
Emission (nm)	**Origin**	**As-prepared ZnO**	**ZnO400**	**ZnO700**	**ZnO900**
Green	V_{Zn} [5],[11],[10]	2.91			6.89
495 – 570		525 nm			514 nm
Yellow – Orange	Excess oxygen[14],[15],	22.71	17.59	14.52	44.22
570 – 620	O_i[16] or other complex defects[17],[15]	572 nm	575 nm	585 nm	605 nm
Red	$O_{i\ (oct)}^{2-}$ defect[5]	70.25	58.32	75.79	2.81
620 – 750		654 nm	654 nm	670 nm	649 nm
NIR	Radiative recombination of shallow donor with deep acceptor O_i[18]		11.85	1.46	36.49
			734 nm	734 nm	711 nm
Infrared emission	$O_{i\ (oct)}^{-}$ [5]	4.01	12.52	8.18	9.65
		823 nm	787 nm	822 nm	825 nm

3.3. Photocatalytic activity

Photocatalytic activities of hydrothermal ZnO samples were evaluated by the degradation of Methylene blue (MB, ≥ 99%, Jinhuada) $C_{16}H_{18}ClN_3S.3H_2O$ (M = 373.90 g.mol^{-1}), a redox indicator used in chemical analysis, which has the most dominant peak at 664 nm. This solution is discolored in the redox environment. Hence, MB is often used to evaluate the photocatalytic ability of materials. The measurement process was as followed. Firstly, MB was dissolved in 1L of distilled water stored in a 1500 mL volumetric flask in a dark room to obtain a concentration C = 25.10^{-6} (mol.L^{-1}). Then, 20 mg of ZnO materials were added in 250 mL MB solution under vigorous stirring for 60 mins in dark at room temperature to get adsorption equilibrium. Finally, the solution was under direct sunlight irradiation and UV-Vis absorption measurement (DR 5000) was recorded after every 30 min of irradiation until 150 min. The photocatalytic efficiency for MB degradation could be calculated as [19]:

$$\eta(\%) = (1 - \frac{C}{C_0}) \times 100\%$$

where C_0 is the MB initial absorption value, and C is the MB absorption value at each time of measurement.

The absorption spectra of ZnO400 and ZnO700 were shown in Fig. 5. As one can see, the photocatalytic activity of ZnO improves when ZnO was annealed at 700^{o}C. Fig. 6 showed the MB degradation at the most dominant peak (664 nm). After 150 min, the photocatalytic efficiencies of ZnO, ZnO400, and ZnO700 were 21%, 48%, and 79%, respectively. Then the thermal annealing has a great effect on photocatalytic activity of ZnO. When increasing the annealing temperature of ZnO until 700^{o}C, the PL intensity was increased routinely. Thus, the interaction of excited electrons in the environment was increased in the sample with higher annealed temperature which could be a reason to enhance the photocatalytic activity.

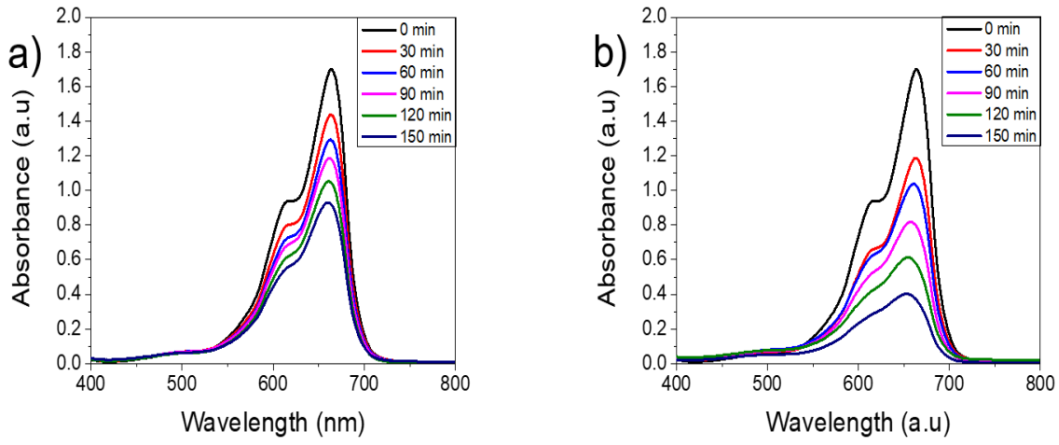

Figure 5. The schematic of the adsorption, photocatalytic activities of ZnO400 and ZnO700 prepared by hydrothermal method and examined for 150 min with MB as the color indicator: a) ZnO400 and b) ZnO700.

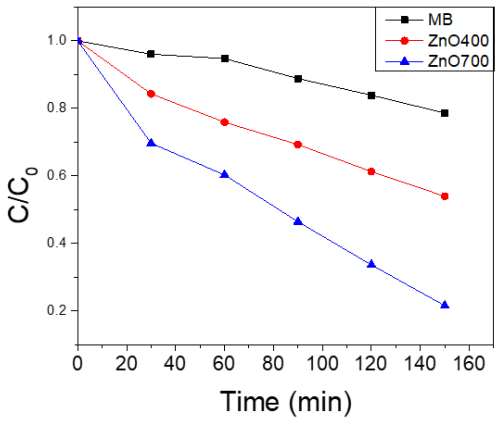

Figure 6. Methylene blue degradation at 664 nm under sunlight irradiation of ZnO(MB), ZnO400, and ZnO700.

4. Conclusions

In this study, homogeneous wurtzite ZnO nanorods were synthesized by a facile hydrothermal method. The resulted sample was annealed in air at different temperatures 400, 700, and 900°C. The photoluminescence emission spectra of these samples showed that the intensity of the visible-range emission was increased with the temperature increased until 700°C. The PL line shape of these samples was similar to each other indicating that they have the same emission origin. However, the deconvolution of PL emissions showed that the proportions of emission peaks were different. The photocatalytic activities of the samples in the degradation of MB solution have been evaluated and this showed that the higher intensity of PL emission gave better photocatalytic activity.

Acknowledgements

This research is funded by Vietnam National Foundation for Science and Technology Development (NAFOSTED) under Grant Number 103.02-2016.87

References

[1] F. Achouri, S. Corbel, L. Balan, K. Mozet, E. Girot, G. Medjahdi, M.B. Said, A. Ghrabi, R. Schneider, Porous Mn-doped ZnO nanoparticles for enhanced solar and visible light photocatalysis, Mater. Des., 101 (2016) 309-316. https://doi.org/10.1016/j.matdes.2016.04.015

[2] S. Choi, J.Y. Do, J.H. Lee, C.S. Ra, S.K. Kim, M. Kang, Optical properties of Cu-incorporated ZnO (Cu x Zn y O) nanoparticles and their photocatalytic hydrogen production performances, Mater. Chem. Phys., 205 (2018) 206-209.
https://doi.org/10.1016/j.matchemphys.2017.11.022

[3] X.M. Fan, J.S. Lian, L. Zhao, Y.H. Liu, Single violet luminescence emitted from ZnO films obtained by oxidation of Zn film on quartz glass, Appl. Sur. Sci., 252 (2005) 420-424.
https://doi.org/10.1016/j.apsusc.2005.01.018

[4] C.T. Quy, N.X. Thai, N.D. Hoa, D.T.T. Le, C.M. Hung, N.V. Duy, N.V. Hieu, C_2H_5OH and NO_2 sensing properties of ZnO nanostructures: correlation between crystal size, defect level and sensing performance, RSC Adv., 8 (2018) 5629-5639.
https://doi.org/10.1039/C7RA13702H

[5] A. Janotti, C.G. van de Walle, Native point defects in ZnO, Phys. Rev. B, 76 (2007) 165202.
https://doi.org/10.1103/PhysRevB.76.165202

[6] K. Vanheusden, C.H. Seager, W.L. Warren, D.R. Tallant, J.A. Voigt, Correlation between photoluminescence and oxygen vacancies in ZnO phosphors, Appl. Phys. Lett., 68 (1996) 403.
https://doi.org/10.1063/1.116699

[7] K. Vanheusden, C. H. Seager, W.L. Warren, D.R. Tallant, J. Caruso, M.J. Hampden-Smith, T.T. Kodas, Green photoluminescence efficiency and free-carrier density in ZnO phosphor powders prepared by spray pyrolysis, J. Lumin., 75 (1997) 11-16.
https://doi.org/10.1016/S0022-2313(96)00096-8

[8] F.H. Leiter, H.R. Alves, A. Hofstaetter, D.M. Hofmann, B.K. Meyer, The Oxygen Vacancy as the Origin of a Green Emission in Undoped ZnO, Phys. Status Solidi (b), 226 (2001) R4-R5.
https://doi.org/10.1002/1521-3951(200107)226:1<R4::AID-PSSB99994>3.0.CO;2-F

[9] F. Leiter, H. Alves, D. Pfisterer, N.G. Romanov, D.M. Hofmann, B.K. Meyera, Oxygen vacancies in ZnO, Physica B: Condens. Matter, 340-342 (2003) 201-204.
https://doi.org/10.1016/j.physb.2003.09.031

[10] D.C. Reynolds, D.C. Look, B. Jogai, J.E. Van Nostrand, R. Jonesb, J. Jennyb, Source of the yellow luminescence band in GaN grown by gas-source molecular beam epitaxy and the green luminescence band in single crystal ZnO, Solid State Commun., 106 (1998) 701-704.
https://doi.org/10.1016/S0038-1098(98)00048-9

[11] A.F. Kohan, G. Ceder, D. Morgan, C.G. Van de Walle, First-principles study of native point defects in ZnO, Phys. Rev. B, 61 (2000) 15019.
https://doi.org/10.1063/1.3089232

[12] T. Sekiguchi, N. Ohashi, Y. Terada, Effect of Hydrogenation on ZnO Luminescence, Jpn. J. Appl. Phys., 36 (1997) 289-291.
https://doi.org/10.1143/JJAP.36.L289

[13] E.V. Lavrov, J. Weber, F. Börrnert, Chris G. Van de Walle, R. Helbig, Hydrogen-related defects in ZnO studied by infrared absorption spectroscopy, Phys. Rev. B, 66 (2002) 165205.
https://doi.org/10.1103/PhysRevB.66.165205

[14] Y.Y. Tay, T.T. Tan, F. Boey, M.H. Liang, J. Ye, Y. Zhao, T. Norby, S. Li, Correlation between the characteristic green emissions and specific defects of ZnO, Phys. Chem. Chem. Phys., 12 (2010) 2373-2379
https://doi.org/10.1039/b922372j

[15] M. S. Ramanachalam, A. Rohatgi, W. B. Carter, J. P. Schaffer, T. K. Gupta, Photoluminescence study of ZnO varistor stability, J. Electron. Mater., 24 (1995) 413-419.
https://doi.org/10.1007/BF02659707

[16] M. Willander, O. Nur, J.R. Sadaf, M.I. Qadir, S. Zaman, A. Zainelabdin, N. Bano, I. Hussain, Luminescence from Zinc Oxide Nanostructures and Polymers and their Hybrid Devices, Materials, 3 (2010) 2643-2667.
https://doi.org/10.3390/ma3042643

[17] A.B. Djurisic, X.Y. Chen, H.Y. Leung, Recent Progress in Hydrothermal Synthesis of Zinc Oxide Nanomaterials, Recent Pat. Nanotechnol., 6 (2012) 124-134(111).
https://doi.org/10.2174/187221012800270180

[18] M. Wang, Y. Zhou, Y. Zhang, E.J. Kim, S.H. Hahn, S.G. Seong, Near-infrared Photoluminescence from ZnO, Appl. Phys. Lett., 100 (2012) 101906. https://doi.org/10.1063/1.3692584

[19] N.X. Sang, P.T.L. Huong, T.T.M. Thy, P.T. Dat, V.C. Minh, N.H. Tho, Crystalline deformation and photoluminescence of titanium dioxide nanotubes during in situ hybridization with graphene: An example of the heterogeneous photocatalyst, Superlattice. Microst., 121 (2018) 9-15. https://doi.org/10.1016/j.spmi.2018.07.020